molecular pharmaceutics

Article

Cite This: *Mol. Pharmaceutics* XXXX, XXX, XXX−XXX

Optimization of a Protease Activated Probe for Optical Surgical Navigation

Joshua J. Yim,[†,‡] Martina Tholen,[‡,§] Alwin Klaassen,[∥] Jonathan Sorger,[∥] and Matthew Bogyo*[,†,§,⊥]

[†]Department of Chemical and Systems Biology, [§]Department of Pathology, and [⊥]Department of Microbiology and Immunology, Stanford University School of Medicine, 300 Pasteur Drive, Stanford, California 94305, United States

[∥]Intuitive Surgical Inc., 1020 Kifer Road, Sunnyvale, California 94086, United States

Supporting Information

ABSTRACT: Molecularly targeted optical contrast agents have the potential to enable surgeons to visualize specific molecular markers that can help improve surgical precision and thus outcomes. Fluorescently quenched substrates can be used to highlight tumor lesions by targeting proteases that are highly abundant in the tumor microenvironment. However, the majority of these and other molecularly targeted optical contrast agents are labeled with reporter dyes that are not ideally matched to the properties of clinical camera systems, which are typically optimized for detection of indocyanine-green (ICG). While a wide range of near-infrared (NIR) dyes are suitable for use with highly sensitive and highly tunable research-focused small animal imaging systems, most have not been evaluated for use with commonly used clinical imaging systems. Here we report the optimization of a small molecule fluorescently quenched protease substrate probe 6QC-ICG, which uses the indocyanine green (ICG) dye as its optical reporter. We evaluated dosing and kinetic parameters of this molecule in tumor-bearing mice and observed optimal tumor over background signals in as little as 90 min with a dose of 2.3 mg/kg. Importantly, the fluorescence intensity of the probe signal in tumors did not linearly scale with dose, suggesting the importance of detailed dosing studies. Furthermore, when imaged using the FDA approved *da Vinci* Si surgical system with Firefly detection, signals were significantly higher for the ICG probe compared to a corresponding probe containing a dye with similar quantum yield but with a slightly shifted excitation and emission profile. The increased signal intensity generated by the optimal dye and dose of the ICG labeled probe enabled detection of small, flat lesions that were less than 5 mm in diameter. Therefore, 6QC-ICG is a highly sensitive probe that performs optimally with clinical imaging systems and has great potential for applications in optical surgical navigation.

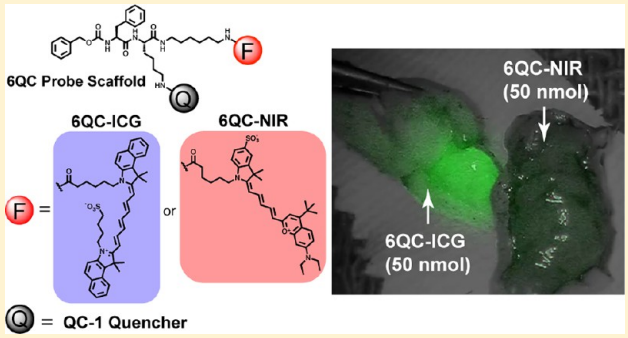

KEYWORDS: *optical contrast agents, fluorescently quenched probes, fluorescence guided surgery*

INTRODUCTION

Despite advances in chemotherapy and radiation therapy, surgical resection still remains the primary method to treat most solid tumors.[1,2] Surgeons rely on their visual and tactile assessment of cancerous lesions to define resection borders. The inability to accurately assess these margins between tumor and healthy tissues in real time results in incomplete removal of tumor tissue (up to 30−65% of cases)[3−5] or leads to excess removal of healthy tissue. Fluorescence guided surgery (FGS) has the potential to greatly improve surgical resections by using fluorescent agents during surgical procedures that improve intraoperative decision-making.[6,7] However, currently, there are only a few fluorescent agents approved by the FDA for clinical use.[6] Indocyanine green (ICG), the only FDA-approved NIR fluorophore,[6] is a nontargeted dye used for monitoring blood flow[8] and tissue perfusion,[9,10] as well as for some gastrointestinal imaging applications.[11,12] ICG has also been used to identify cancer via sentinel lymph node mapping[13] and leaky vasculature accumulation[14] in tumors. Consequently, all FDA-approved clinical NIR fluorescence imagers have been tuned to the ICG excitation/emission wavelength (ex/em = 805/835 nm)[12,15] which is outside the absorption range of hemoglobin and water and within the "optical window" (650−900 nm) for *in vivo* fluorescence imaging.[16]

A number of strategies have been exploited to functionalize optical imaging reporters to achieve tumor-specific contrast.[17] Fluorescent dyes can be coupled to small molecules or protein-based ligands that bind with high affinity to tumor specific proteins, such as tumor cell surface receptors (reviewed in ref 17). Alternatively, the activity of tumor-specific enzymes can be exploited to generate signals only at a site of interest. Proteases have become the enzymes of choice for this strategy because short peptide substrates can be decorated with suitable

Special Issue: Pharmacology by Chemical Biology

Received: September 19, 2017
Revised: November 17, 2017
Accepted: November 25, 2017
Published: November 25, 2017

DOI: 10.1021/acs.molpharmaceut.7b00822
Mol. Pharmaceutics XXXX, XXX, XXX−XXX

fluorophore/quencher pairs such that probes are optically silent until cleaved by a protease.[18−22] These quenched substrates have an advantage over affinity probes because they do not require clearance of free probe to produce high contrast thus enabling rapid imaging workflows.

Multiple proteases have proven to be useful biomarkers of cancerous tissues.[23−26] We have shown that cysteine cathepsins, a class of lysosomal cysteine proteases, are highly expressed in activated macrophages found in the tumor microenvironment and thus can be used to specifically detect tumor tissues.[22,27,28] These tumor associated macrophages (TAMs) produce high proteolytic activity required for tissue remodeling, initiation of angiogenesis, and invasion of the tumor.[25,29,30] Previously, our group designed a cysteine cathepsin cleavable NIR substrate probe 6QC-NIR[22] using the commercially available fluorophore Dylight 780-B1. Cleavage of this substrate probe produces high tumor signals in cancers of the lung, breast, and colon, which could be detected with the FDA-approved *da Vinci* Si surgical system (Intuitive Surgical) equipped with the Firefly imaging system.[22] However, this dye, while similar in structure and photochemical properties to the clinically used ICG dye, has slightly shifted excitation and emission peaks and produced relatively weak signals when imaged in Firefly mode. We therefore wanted to test the impact of the fluorophore on the probe and furthermore to determine the optimal probe dose to produce maximal fluorescent signals in the tumor. We show here that changing the fluorophore from Dylight 780-B1 to ICG resulted in a significant increase in fluorescent signal within the tumor and that this boost in signal was not the result of changes in overall probe distribution. Furthermore, dosing studies showed a nonlinear response with high probe doses resulting in reduced signal likely due to proximity induced quenching of the dye in the tumor tissues. By optimizing the dye properties to match the camera system and using an optimal dose of probe, we were able to detect tumor margins in lesions as small as 3 mm in diameter in as short as 90 min after probe administration, making this agent highly valuable for translation into the clinic.

RESULTS

Design and Synthesis of 6QC-ICG. We previously developed both substrate[22] and covalent[28] probes for cysteine cathepsins using a core Cbz-Phe-Lys peptide sequence. The substrate probe 6QC-NIR is functionalized with a Dylight 780-B1 fluorophore attached to the peptide by a six carbon alkyl linker and a NIR quencher, QC-1, conjugated to the lysine side chain (Figure 1). Upon cleavage of the substrate amide bond by cathepsins, two fragments are produced. The fragment containing the fluorescent reporter is released with a free amine that can be protonated in the acidic lysosome, leading to its accumulation (Figure 1). This latent lysosomotropic effect (LLE) results in fluorescent signals that accumulate in tumor tissue rather than being rapidly cleared through circulation.

We first evaluated how efficiently several clinical camera systems detected the Dylight 780-B1 dye compared to ICG. We compared a dilution series of the free ICG and Dylight 780-B1 dyes imaged using the FDA approved *da Vinci* Si Firefly system (Intuitive Surgical) and the SPY Elite camera (NOVADAQ Technologies). We compared these to images taken using the Pearl Trilogy imager (LI-COR Biosciences), a small animal imaging system that is only used for preclinical animal studies (Figure 2A). Within the dynamic range of the imagers tested, the detection thresholds were 10−100 times more sensitive for

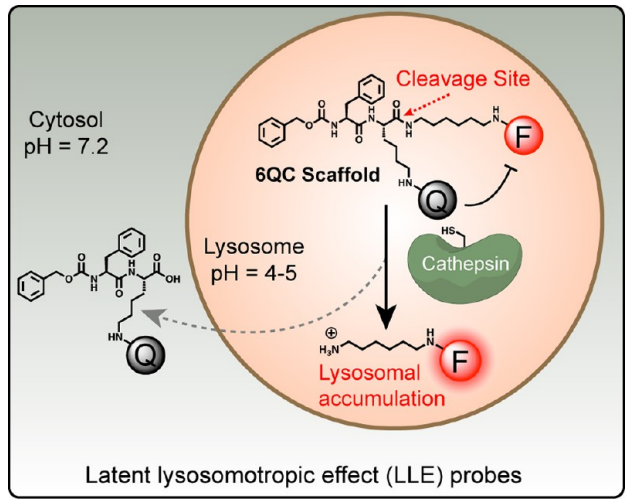

Figure 1. Schematic representation of the latent lysosomotropic effect that results in fluorophore retention of the fluorescent product in the lysosome upon cleavage by cysteine cathepsins.

ICG compared to Dylight 780-B1. It is worth noting that maximal ICG and Dyight780-B1 fluorescence was observed at 10 μM and 100 μM respectively, suggesting self-quenching effects of the dyes at higher concentrations, also seen *in vivo*.[31] Importantly, by adjusting the gain setting of the camera on the Pearl Trilogy, it was possible to detect quantifiable fluorescent signals for the ICG dye at 1000 times lower dye concentrations than when using either clinical camera system. This demonstrates that optimization of imaging probes using highly sensitive research-only camera systems is not necessarily a good surrogate for how the probe will perform using clinical imaging systems. Given the enhanced sensitivity of all the camera systems for ICG, we generated a substrate probe where we replaced the Dylight 780-B1 dye with an analogue of ICG that contains a carboxylic acid for conjugation to the Cbz-Phe-Lys scaffold via the lysine side chain (Figure 2B). We synthesized this 6QC-ICG probe using a combination of solid- and solution-phase chemistry as outlined in previous work.[22]

Evaluation of 6QC-ICG for Imaging Tumors *In Vivo*. To compare the effects of changing the fluorophore, we tested 6QC-ICG in the 4T1 orthotopic breast cancer tumor mouse model that was used for the prior studies with 6QC-NIR.[22] Ten days after tumor cell inoculation, we intravenously injected 10 or 50 nmol of either 6QC-NIR or 6QC-ICG and then imaged the animals at various time points over 24 h using the Pearl Trilogy imaging system. Mice treated with the 6QC-ICG probe showed substantially more fluorescence in the tumor than mice injected with 6QC-NIR (example in Figure 3A). The fluorescence intensity at 24 h was 4.4-fold higher for 6QC-ICG compared to 6QC-NIR for the 10 nmol dose and 3.2-fold higher for the 50 nmol dose (Figure 3B). The kinetics of probe labeling showed a steep increase in signal in the first 8 h, followed by a plateau-like phase until the 24 h time point for both probes, resembling the previously reported data for 6QC-NIR.[22] The difference in brightness of the fluorescent signal for the two probes was substantial, with the signal from 6QC-ICG already brighter at 1 h (1.18 AU for 50 nmol) than that of 6QC-NIR after 24 h (1.04 AU for 50 nmol). Interestingly, the observed increase in brightness for the ICG probe did not result in significantly improved tumor signal over background as both 6QC-NIR and 6QC-ICG showed comparable values

DOI: 10.1021/acs.molpharmaceut.7b00822
Mol. Pharmaceutics XXXX, XXX, XXX−XXX

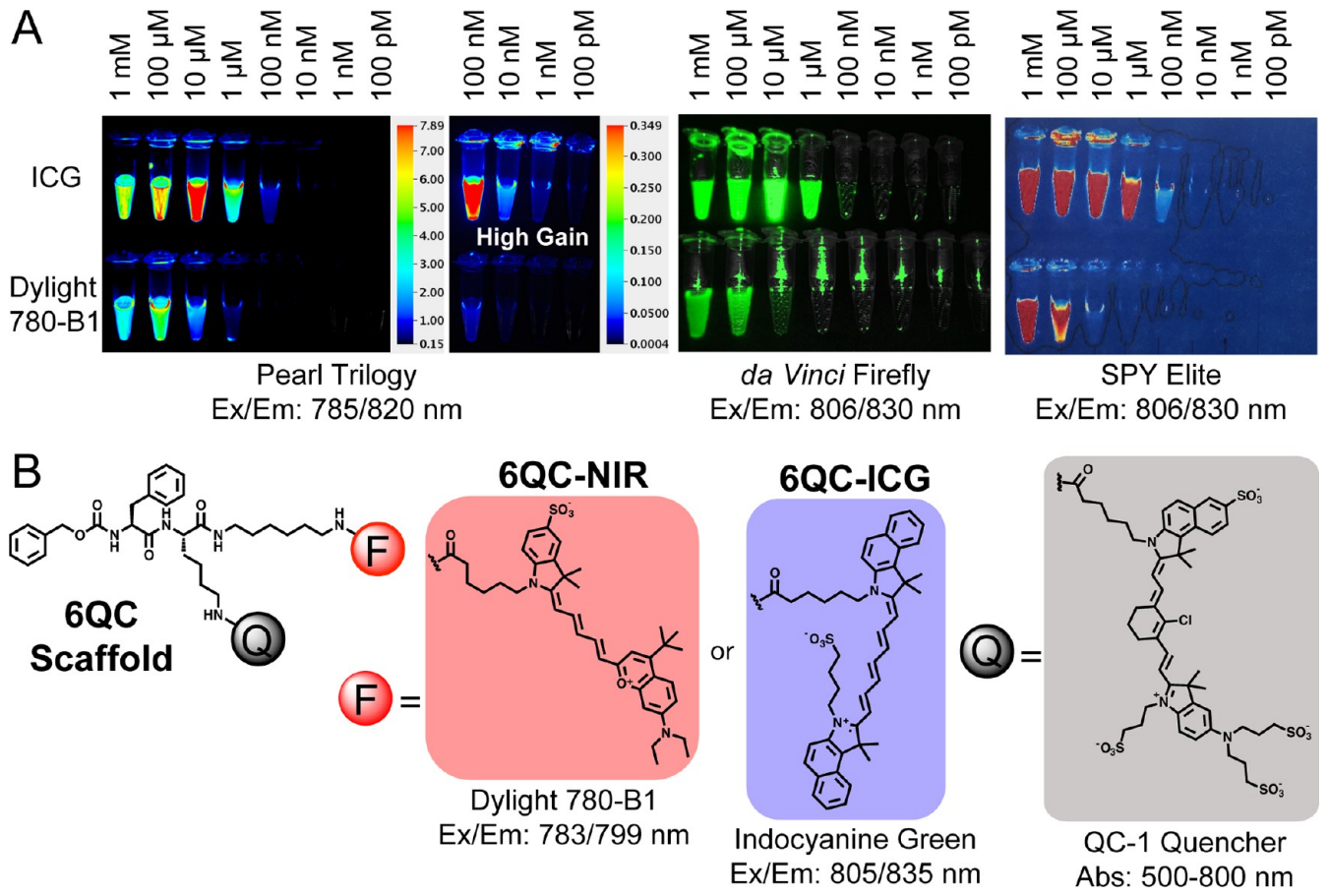

Figure 2. (A) Indocyanine green (ICG) and Dylight 780-B1 acid serial dilution in DMSO under clinical and preclinical imagers. Snapshots from Pearl Trilogy (LI-COR Biosciences), *da Vinci* Firefly (Intuitive Surgical), and SPY Elite (NOVADAQ Technologies) systems. (B) Chemical structure of 6QC-NIR and 6QC-ICG functionalized with respective fluorophores and QC-1 quencher.

(Figure 3C). It is noteworthy that tumor signal over background values stays relatively constant over time, suggesting that while imaging at later time points may increase overall signal intensity, it may not necessarily dramatically improve signal over background values. Furthermore, we compared fluorescence of the tumor to the following organs: fat pads, kidneys, liver, and the intestines for the two probes 6QC-NIR and 6QC-ICG (Figure 3D). This data suggests that there are no substantial changes in overall biodistribution due to the change in probe fluorophore. Similar to the 6QC-NIR, 6QC-ICG shows high fluorescence in the kidneys and intestines. Kidneys are known to express high levels of cathepsins causing the strong signal[32] while the signal in the intestine is mainly due to excretion of cleaved probe (data not shown).

Kinetics of 6QC-ICG Activation at Early Time Points. One of the most significant advantages of using an activatable "smart probe" such as 6QC-ICG is that the probe produces signal only when processed by the target enzymes, allowing it to be used for rapid imaging application. We therefore wanted to carefully examine the kinetics of probe activation over the first 2 h after administration. This time window was selected to allow for probe administration immediately prior to the start of a surgical procedure, limiting impact on surgical workflow. Therefore, we injected 4T1 tumor-bearing mice with 50 nmol of 6QC-ICG and collected images on the Pearl Trilogy every 5 min for 2 h. These images could then be used to generate a video of real-time signal accumulation in the tumors (Movie S1). Levels of tumor signals could also be carefully quantified over this time window and compared to background tissue signals (Figure 4A). At the 90 min time point, we observed a signal over background contrast of 3.2-fold (Figure S1) which is about 80% of the maximal signal over background observed at 8 h (Figure 3C). This data suggests that the increase in tumor fluorescence that results from the ICG dye substitution allows tumor detection starting at time points as early as 90 min without forfeiting significant contrast or total fluorescence levels that could be obtained at later time points. This data also suggests that the 6QC-ICG probe activation kinetics would be appropriate for administration to patients just prior to surgery.

Dose Studies of 6QC-ICG. Having established a practical time window for imaging, we tested how the dosage of the probe affects signal intensity *in vivo*. We injected 4T1 tumor-bearing mice with doses of 6QC-ICG ranging from 6.25 nmol to 100 nmol, corresponding to 0.58 mg/kg to 9.2 mg/kg, and collected images of the tumors at 90 min (Figure S2). We initially thought that increasing the dose of 6QC-ICG would yield a brighter signal due to increased substrate turnover. However, our results indicated that the signal intensity of the tumors did not linearly scale with dose of the probe and rather that the middle dose of 25 nmol (2.3 mg/kg) yielded the brightest tumor fluorescence (Figure 4B). This may be due to self-quenching of the probe signal in the tumor once concentrations get too high in those tissues. At a 25 nmol dose, the theoretical probe concentration in the blood is 12.5 μM, assuming a total blood volume of 2 mL. Therefore, the

DOI: 10.1021/acs.molpharmaceut.7b00822
Mol. Pharmaceutics XXXX, XXX, XXX−XXX

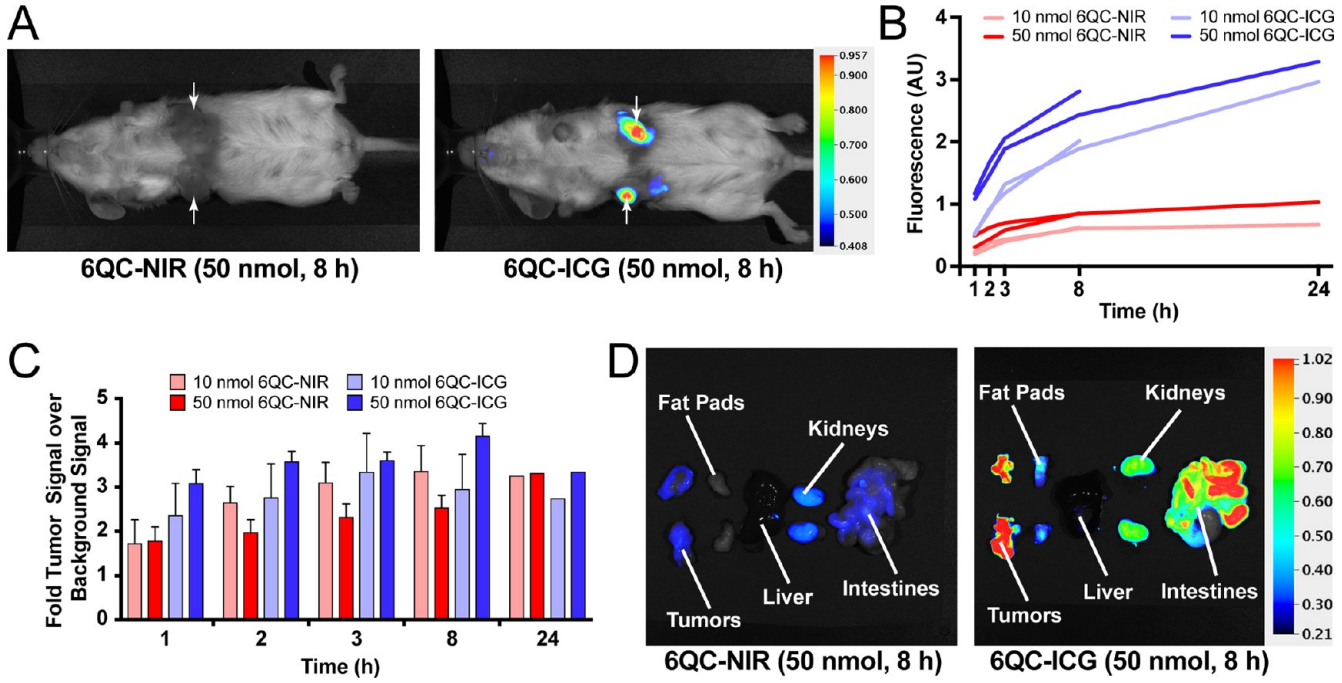

Figure 3. (A) 4T1 tumor-bearing mice injected with 50 nmol of 6QC-NIR or 6QC-ICG and imaged at 8 h (Pearl Trilogy). Images were normalized to the same maximal fluorescence. (B) Time course of 6QC-NIR and 6QC-ICG dosed at 10 nmol and 50 nmol per mouse. Fluorescence measurements at 1, 2, 3, 8, and 24 h (Pearl Trilogy). One animal of each group was sacrificed at 8 h. Each line represents one animal plotting the average fluorescence signal from normalized regions of interest from two tumors. (C) Tumor fluorescence over background fluorescence at various time points. Background fluorescence was measured in the hair free area proximal to the tumor. Mean values ± SD of 4 tumors from two mice each (1−8 h) or two tumors from one mouse (24 h). (D) Normalized images of various organ fluorescence at 8 h after probe injection.

accumulation of the cleaved 6QC-ICG in the tumor tissue may reach self-quenching concentrations (Figure 2A and Figure S3). Previous studies have shown that ICG at 5−10 mg/kg accumulates in the tumor site due to enhanced permeability and retention (EPR) in those tissues.[33] These are much higher doses than the clinical dose of around 0.1 mg/kg used for imaging vasculature.[34] Therefore, we also wanted to confirm that tumor signals from our probe injected mice were not the result of general EPR effects. Treatment of 4T1 tumor-bearing mice with either 10 nmol (0.9 mg/kg) or 100 nmol (9.2 mg/kg) of free ICG dye did not result in any significant accumulation of fluorescent signal in the tumor (Figure S4), confirming that the rapidly produced signal from 6QC-ICG in tumors was the result of activation of the probe by proteases in the tumor microenvironment.

Application of 6QC-ICG Probe in FGS Using the *da Vinci* Surgical System. After having conducted our initial studies using the Pearl Trilogy imaging system which allows careful quantification of fluorescent signals, we wanted to test our optimized probe using the FDA approved *da Vinci* Si surgical system outfitted with a NIR Firefly camera. Previous studies of 6QC-NIR using this system showed reasonable tumor contrast at 6 h after probe injection.[22] To compare the 6QC-ICG probe to 6QC-NIR, we used the same syngeneic 4T1 breast cancer mouse model and probe dose (50 nmol) from the prior study but conducted fluorescence guided surgery at 90 min post probe injection. Imaging of the subcutaneous tumor fluorescence prior to initial incision confirmed a substantial fluorescence signal boost for 6QC-ICG probe compared to the original 6QC-NIR probe (Figure 5A). This boost in intensity was even more pronounced when excised tumors were removed surgically (Figure 5B). Furthermore, to visualize a fluorescent signal in tumors for mice treated with the original 6QC-NIR probe at 90 min post injection, we had to increase the camera gain setting on the Firefly system, leading to a large increase in noise that limited the utility of this probe for real time surgical guidance. However, the substantially higher tumor fluorescence resulting from the 6QC-ICG probe allowed us to conduct fluorescence-guided surgery with clear detection of the tumor and low background signals from the healthy tumor bed (Figure 5C and Movie S2). Our studies with the *da Vinci* Si surgical system suggest that the signal increase from the dye change allows the Firefly camera system to detect the tumor and surrounding tissue with high precision, translating into improved tumor recognition for more accurate tumor removal.

Sensitivity of 6QC-ICG for Detection of Tumor Tissues *In Vivo*. The 4T1 breast cancer mouse model usually involves injection of 50,000 cells or more at a single site, resulting in visible tumors as early as 7 days after injection. These rather large lesions, which are often around 1 cm in diameter, give strong tumor fluorescent signal in mice injected with the 6QC-ICG probe (for example in Figures 4C and 4D). However, for clinical applications, it is important to understand how sensitively the probe can detect smaller, flat lesions derived from a smaller number of tumor cells. This is particularly relevant for clinical decision making during surgery since the purpose of FGS is to increase the sensitivity for detecting fine margins in often diffusely growing tumors and to make intraoperative assessments of potentially small metastatic lesions. In order to produce tumors that would more accurately mimic a small clinical lesion, we reduced the number of 4T1 cells injected by 10-fold and imaged the mice after only 8 days of growth. With only 5,000 cells used for seeding, tumors were

DOI: 10.1021/acs.molpharmaceut.7b00822
Mol. Pharmaceutics XXXX, XXX, XXX−XXX

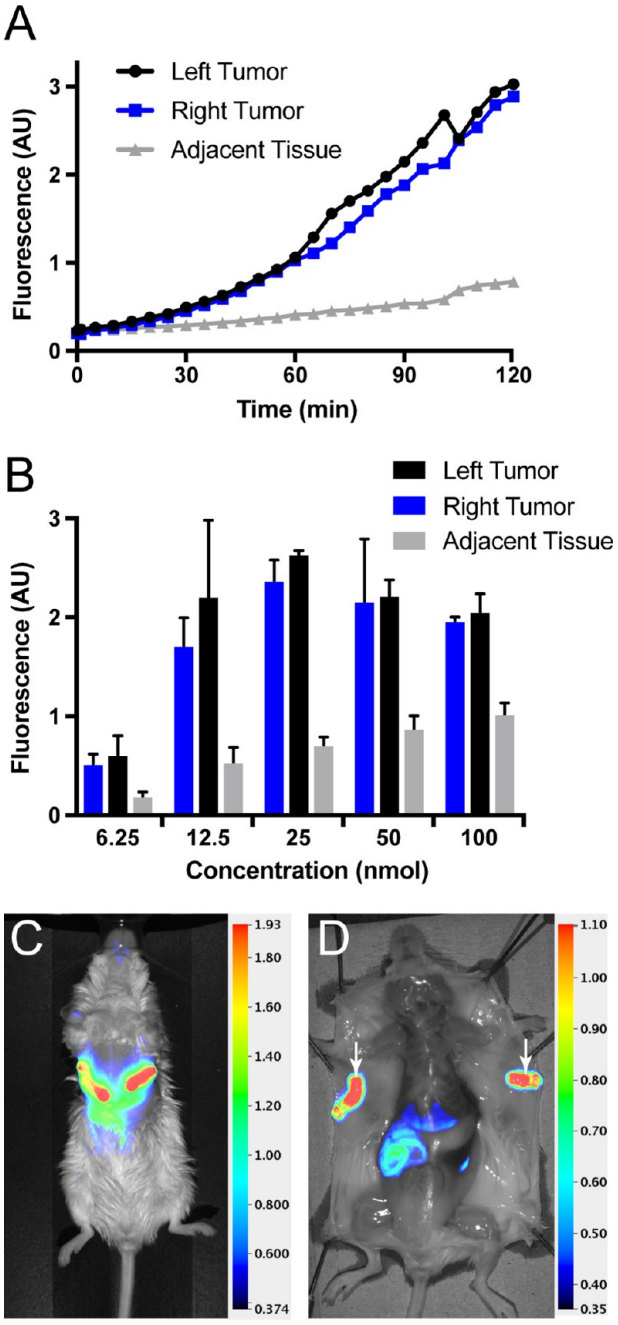

Figure 4. (A) Fluorescence intensity of tumor and adjacent tissue signals over the first 2 h after injection of 50 nmol of 6QC-ICG; $n = 1$. (B) Fluorescence of tumors and adjacent tissue at varying doses of 6QC-ICG imaged at 90 min. Mean values ± SD ($n = 3$ for 6.25 and 100 nmol; $n = 4$ for 12.5, 25, and 50 nmol). Fluorescence values taken from normalized region of interest in tumor and adjacent tissue. (C) 4T1 tumor-bearing mouse injected with 25 nmol of 6QC-ICG and imaged at 90 min and (D) splayed open post-mortem at 2 h.

not detectable by simple visible examination and palpation of the animals. Additionally, these animals injected with 25 nmol of 6QC-ICG and imaged with the Pearl Trilogy did not show any subcutaneous fluorescent signal. However, when the surgically opened site was directly analyzed post-mortem, we were able to clearly detect a fluorescent signal in the region of the tumor (Figure 6A, right panel). On closer examination in white light and under fluorescence, the signal corresponded to two distinct regions (Figure 6B, first and second panels to the left). Region 1 presented as a lymph node in white light as well as in subsequent histology of the excised tissue (third and fourth panels). Region 2 was approximately 3 mm in size and did not present as an embossed tumor mass but showed a slight increase in vasculature in this area. Histological analysis confirmed the excised tissue from region 2 to be cancerous, as the details show disordered structure and tumor cell masses infiltrating muscle tissue. These studies show that the 6QC-ICG probe has the capability to highlight extremely small tumor lesions. With the improved fluorescent signal from ICG conjugation, detection of early initial tumor sites, as well as metastasized secondary sites, can be highlighted with high spatial accuracy.

DISCUSSION

Fluorescence guided surgery (FGS) is a relatively new technique that has the potential to greatly improve surgical precision and overall patient outcomes. The success for future implementation of FGS into standard surgical workflows will require significant advances in the development of optical contrast agents. Currently, the only FDA approved NIR fluorescent agent that can be used for clinical imaging applications is the general vascular dye ICG. While this dye is widely used for a number of applications, it has significant limitations due to the fact that it does not provide any information about specific molecular disease markers. While there have been recent advances in the design and implementation of new targeted NIR optical agents,[17] most of these have been validated using preclinical studies in animal models of disease. These preclinical studies use highly sensitive camera systems that can be tuned to a specific dye excitation and emission profile allowing detection of low concentrations of a range of fluorophores. However, as more optical probes are being translated into clinical applications,[17] it becomes important to understand how specific contrast agents perform with FDA approved camera systems that are currently used in surgical suites around the world. Furthermore, a clear understanding of optimal dosing (i.e., administration route, dose, and timing) will be required to accurately and efficiently allow surgeons to use FGS to guide tumor resection.

In this study, we describe our efforts to convert a first generation "smart probe" for protease activity associated with the tumor microenvironment into a probe that is optimized for use with current clinical imaging systems. This involved replacement of the Dylight 780-B1 reporter dye on the previously published probe 6QC-NIR with ICG to more closely match the capabilities of current clinical camera systems. We evaluated applicable time and dosing parameters of 6QC-ICG in mice and found that, 90 min after probe injection, we observed clear tumor signal over background tissue signal, suggesting that this probe could be administered on the day of surgery in a clinical setting. Interestingly, we found that 2.3 mg/kg was the optimal dose while higher doses did not increase the signal, suggesting that dye accumulation in tumors may cause the fluorescent signal to self-quench. Our findings indicate that simply increasing the dose of fluorescent contrast agents may not be an optimal strategy when trying to increase overall brightness of the tumor. Future clinical studies will be needed to see how well the dosing parameters described here translate from mice to humans.

Our studies also demonstrate the importance of employing fluorophore/quencher pairs that are matched with the imaging system being used. Comparing 6QC-ICG to 6QC-NIR, we

DOI: 10.1021/acs.molpharmaceut.7b00822
Mol. Pharmaceutics XXXX, XXX, XXX−XXX

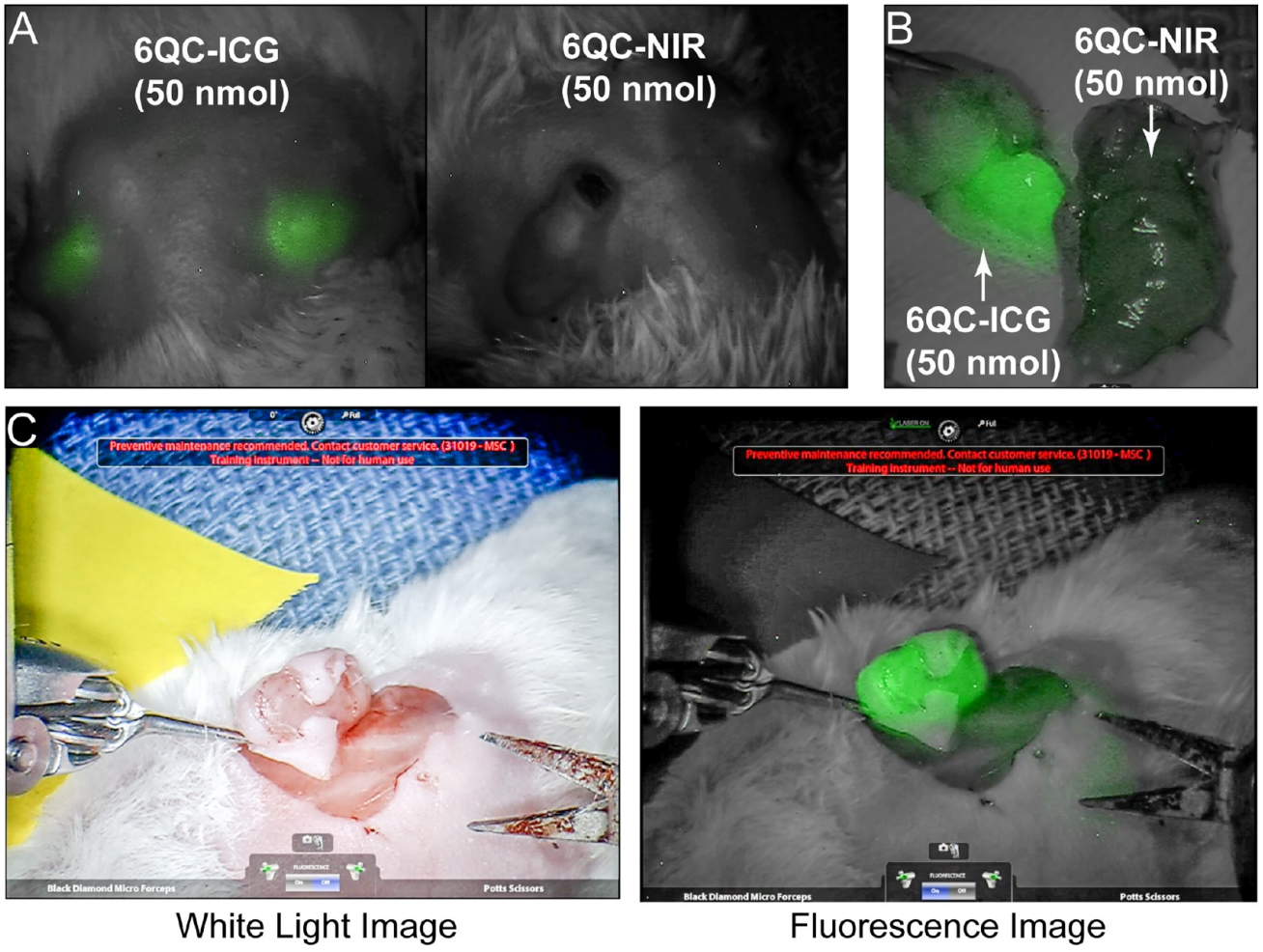

Figure 5. (A) Screen capture of *da Vinci* Si Firefly fluorescence of 4T1 tumor-bearing mice 90 min after injection with 6QC-ICG (left) or 6QC-NIR (right). (B) Screen capture of tumors excised from 4T1 tumor-bearing mice 90 min after injection with 6QC-ICG (left) or 6QC-NIR (right). (C) Screen capture of tumor and tumor bed with white light illumination (left) and corresponding fluorescence (right) in 6QC-ICG injected animal during surgery.

observed similar fluorescence distribution in various organs as well as *in vivo* probe fluorescence kinetics (Figures 3B and 3D). These data suggest that while the ratio of tumor signal to background is similar to both probes (Figure 3C), the overall brighter signal resulting from the optimized spectral properties of ICG allows application of 6QC-ICG for FGS using the *da Vinci* surgical system. While the wide dynamic range and longer acquisition times allow the nonclinical Pearl Trilogy system to detect weak fluorescence signals in laboratory samples, current clinical cameras such as the Firefly enabled camera of the *da Vinci* system generally have less sensitive detection thresholds. This is because clinical imagers typically acquire images at 30−60 Hz in order to reduce motion artifacts typical of longer exposure times. In this case, converting the 6QC protease probe to the ICG conjugate enabled the use of the *da Vinci* Firefly enabled camera at time points shortly after probe injection with acceptable camera gain settings.

The increase in signal from the ICG-labeled probe can be attributed to the optical overlap of the ICG reporter with the excitation and emission wavelengths of the imagers. Interestingly the Dylight 780-B1 fluorophore is excited within the wavelength range of the detection cameras (Figure 2A) but misses the maximum emission wavelength of the clinical imagers by only 20−30 nm. Furthermore, both the ICG conjugate and Dylight 780-B1 are similar zwitterionic poly methine dyes with similar molar extinction coefficients.[35,36] Our results suggest that despite these seemingly similar properties of the two dyes and the suboptimal quantum yield of ICG (2.7%),[37] the use of a dye with optimal spectral properties for the employed camera can have a dramatic impact on its utility in the clinical setting. Therefore, ICG and other dyes with more closely matched spectral properties to ICG should be considered for conjugation to targeting moieties for use with current clinical imaging systems.

In conclusion, the studies presented here demonstrate that it is possible to convert an existing, preclinically validated optical contrast agent into an agent optimized for use in a clinical setting. Our studies highlight the need for careful evaluation of optimal dosing and an understanding of clinical camera systems to be used. Once probes are optimized for dye properties and dose, it is possible to begin to define a time window where a given clinical candidate probe could be most effectively used. We found that when optimized, the cathepsin targeted probe 6QC-ICG proved highly compatible with same-day administration of the probe for surgical procedures using the *da Vinci* surgical system. Further work is aimed at optimization of the protease recognition sequence of the probe to help to further

DOI: 10.1021/acs.molpharmaceut.7b00822
Mol. Pharmaceutics XXXX, XXX, XXX−XXX

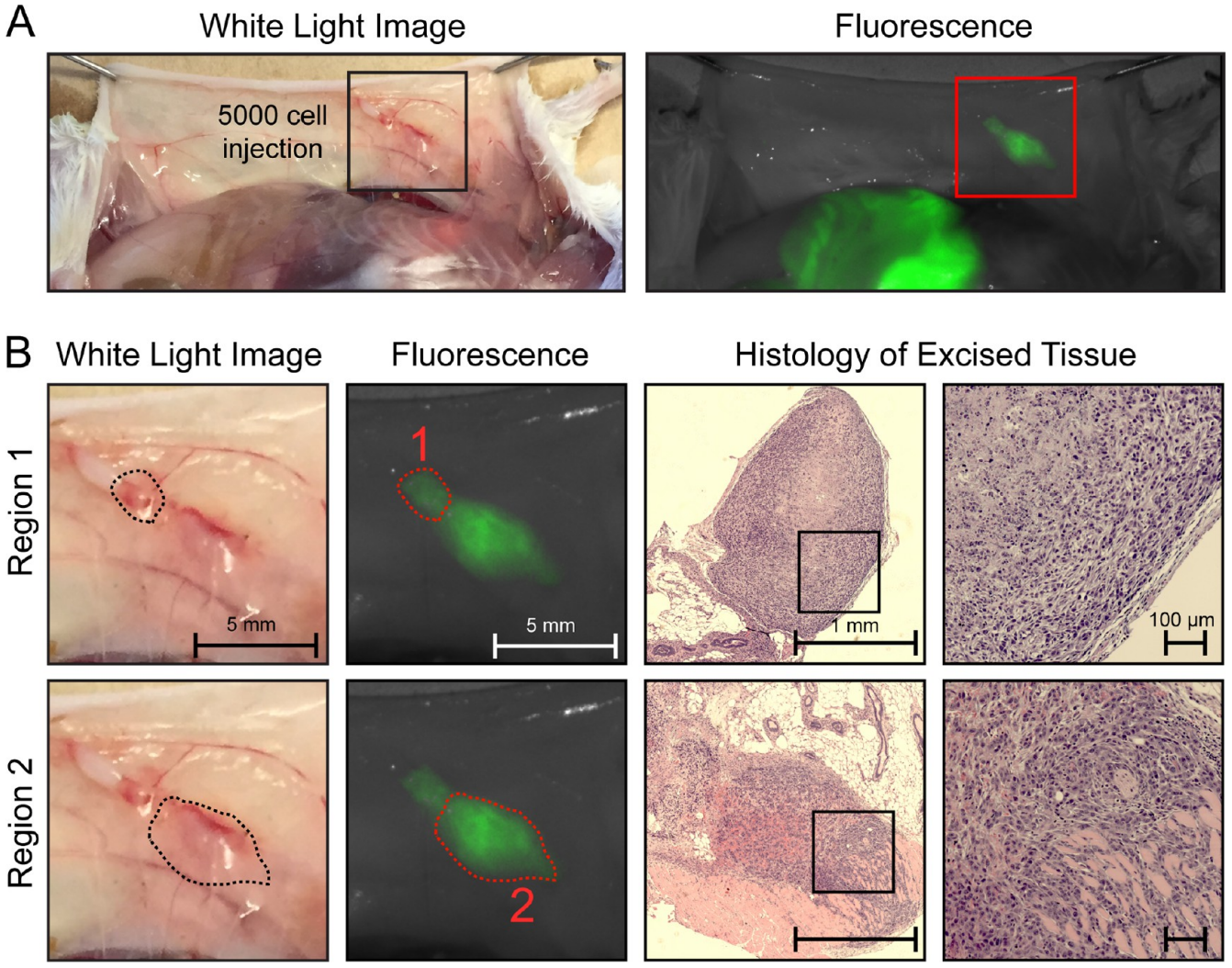

Figure 6. (A) Post-mortem white light and fluorescence images of the region of the mammary fat pad that had been inoculated with 5000 4T1 cells 8 days prior. Images were taken 90 min after injection of 25 nmol of 6QC-ICG using the Pearl Trilogy imaging system. (B) Magnification and histology of the region showing fluorescent signal in the mammary fat pad in panel A. The signal can be assigned to two distinct regions marked with the dotted lines as regions 1 and 2 in the left panels. Histology (in the two right panels) of tissue excised from region 1 shows the characteristic appearance of a lymph node while the histology of region 2 confirms it as a cancerous lesion.

boost signals and reduce the overall background in healthy tissues.

MATERIALS AND METHODS

Compound Synthesis. All reagents and materials used in the synthesis of 6QC-ICG were obtained from commercial sources and used without further purification. IRDye QC-1 NHS ester was purchased from LI-COR Biosciences (Lincoln, Nebraska), and ICG-NHS ester was purchased from Intrace Medical (Lausanne, Switzerland). Compounds were synthesized using reported procedures[22] and purified by reverse phase preparative HPLC. Synthetic procedures including compound characterization are presented in the Supporting Information.

Animal Models. All animal care and experimentation was conducted in accordance with current NIH and Stanford University Institutional Animal Care and Use Committee guidelines.

4T1 cells were implanted into the mammary fat pads of female BALB/c mice (Jackson Laboratory, Bar Harbor, ME). 100 μL of 5×10^4 or 5×10^3 4T1 cells in PBS was injected into mammary fat pads 1 and 10 while the mice were under isofluorane anesthesia. Tumor growth was monitored approximately for 10 days. 10 mM stocks of 6QC-NIR or 6QC-ICG were dissolved in a solution of 10% DMSO in 100 μL of PBS to make solutions ranging from 62.5 μM to 1 mM (range of 6.25–100 nmol per injection) and administered via tail vein.

Mice were imaged noninvasively at indicated time points using the Pearl Trilogy small animal imaging system (LI-COR Biosciences). Signal was detected using the 800 nm filter set. Images were analyzed using Image Studio Software (LI-COR Biosciences). For quantitative analysis of tumor fluorescence signal *in vivo*, signal from a circular region of interest (ROI) of roughly 5 mm in diameter within the tumor or the surrounding tissue was measured. Measured ROI was kept constant in size and tumor region within the same mouse over time.

For *ex vivo* analyses, mice were anesthetized with isofluorane and sacrificed by cervical dislocation. For distribution analyses, tumors and various organs were isolated by dissection. For quantitative analysis of organ fluorescence signal *ex vivo*, ROIs were placed around whole organs, and the total signal was divided by the area of the organ. For post-mortem longitudinal

DOI: 10.1021/acs.molpharmaceut.7b00822
Mol. Pharmaceutics XXXX, XXX, XXX−XXX

display, the sacrificed mice were dissected and the skin pinned open and images were taken.

Histology. Excised tissue underwent standard preparation of paraffin sections and hematoxylin and eosin (H&E) staining.

Intraoperative Fluorescence Guided Surgery with *da Vinci* Si Surgical System. Tumor-bearing mice were administered the indicated probes intravenously (50 nmol in a solution of PBS with 10% DMSO) 90 min prior to surgery. The mice were anesthetized prior to surgery and mounted onto the surgical table under continued anesthesia. Surgery was performed using the *da Vinci* Si surgical system equipped with Firefly fluorescence imaging. Breast cancers were detected with a combination of white and fluorescence light as a guide to determine tumor margins from healthy tissue. Videos of the surgical procedures are available in the Supporting Information (Movie S2).

■ ASSOCIATED CONTENT

Supporting Information

The Supporting Information is available free of charge on the ACS Publications website at DOI: 10.1021/acs.molpharmaceut.7b00822.

Synthetic procedures, compound characterization, and supplemental figures (PDF)

Movies S1 and S2 (ZIP)

■ AUTHOR INFORMATION

Corresponding Author

*E-mail: mbogyo@stanford.edu.

ORCID

Matthew Bogyo: 0000-0003-3753-4412

Author Contributions

‡J.J.Y. and M.T. contributed equally.

Notes

The authors declare the following competing financial interest(s): The authors Jonathan Sorger and Alwin Klaassen are employees and stockholders of Intuitive Surgical Inc.

■ ACKNOWLEDGMENTS

This work was supported by NIH Grants R01 CA179253 and R01 GM111703 (to M.B.), DFG Research Fellowship TH2139/1-1 (to M.T.), and Stanford ChEM-H Chemistry/Biology Interface Predoctoral Training Program and NSF Graduate Research Fellowship Grant DGE-114747 (to J.J.Y.). We thank N. Teraphongphom and R. Ertsey of the Rosenthal laboratory for imaging assistance.

■ REFERENCES

(1) Siegel, R.; DeSantis, C.; Virgo, K.; Stein, K.; Mariotto, A.; Smith, T.; Cooper, D.; Gansler, T.; Lerro, C.; Fedewa, S.; Lin, C.; Leach, C.; Cannady, R. S.; Cho, H.; Scoppa, S.; Hachey, M.; Kirch, R.; Jemal, A.; Ward, E. Cancer treatment and survivorship statistics. *Ca-Cancer J. Clin.* **2012**, *62* (4), 220−41.

(2) Howlader, N., Noone, A. M., Krapcho, M., Miller, D., Bishop, K., Kosary, C. L., Yu, M., Ruhl, J., Tatalovich, Z., Mariotto, A., Lewis, D. R., Chen, H. S., Feuer, E. J., Cronin, K. A., Eds. *SEER Cancer Statistics Review, 1975−2014*; National Cancer Institute: Bethesda, MD, based on November 2016 SEER data submission, posted to the SEER web site, April 2017. https://seer.cancer.gov/csr/1975_2014/.

(3) Yossepowitch, O.; Briganti, A.; Eastham, J. A.; Epstein, J.; Graefen, M.; Montironi, R.; Touijer, K. Positive surgical margins after radical prostatectomy: a systematic review and contemporary update. *Eur. Urol.* **2014**, *65* (2), 303−13.

(4) Winter, J. M.; Cameron, J. L.; Campbell, K. A.; Arnold, M. A.; Chang, D. C.; Coleman, J.; Hodgin, M. B.; Sauter, P. K.; Hruban, R. H.; Riall, T. S.; Schulick, R. D.; Choti, M. A.; Lillemoe, K. D.; Yeo, C. J. 1423 pancreaticoduodenectomies for pancreatic cancer: A single-institution experience. *J. Gastrointest. Surg.* **2006**, *10* (9), 1199−211 and discussion 1210−1.

(5) McGirt, M. J.; Chaichana, K. L.; Attenello, F. J.; Weingart, J. D.; Than, K.; Burger, P. C.; Olivi, A.; Brem, H.; Quinones-Hinojosa, A. Extent of surgical resection is independently associated with survival in patients with hemispheric infiltrating low-grade gliomas. *Neurosurgery* **2008**, *63* (4), 700−7 and author reply 707−8.

(6) Zhang, R. R.; Schroeder, A. B.; Grudzinski, J. J.; Rosenthal, E. L.; Warram, J. M.; Pinchuk, A. N.; Eliceiri, K. W.; Kuo, J. S.; Weichert, J. P. Beyond the margins: real-time detection of cancer using targeted fluorophores. *Nat. Rev. Clin. Oncol.* **2017**, *14* (6), 347−364.

(7) Nguyen, Q. T.; Tsien, R. Y. Fluorescence-guided surgery with live molecular navigation−a new cutting edge. *Nat. Rev. Cancer* **2013**, *13* (9), 653−62.

(8) 510(K) Number K042961. NOVADAQ TECHNOLOGIES, INC.: 2005.

(9) 510(K) Number K063345. NOVADAQ TECHNOLOGIES, INC.: 2007.

(10) 510(K) Number K124031. Intuitive Surgical, Inc.: 2013.

(11) 510(K) Number K100371. NOVADAQ TECHNOLOGIES, INC.: 2011.

(12) DSouza, A. V.; Lin, H.; Henderson, E. R.; Samkoe, K. S.; Pogue, B. W. Review of fluorescence guided surgery systems: identification of key performance capabilities beyond indocyanine green imaging. *J. Biomed. Opt.* **2016**, *21* (8), 80901.

(13) Cousins, A.; Thompson, S. K.; Wedding, A. B.; Thierry, B. Clinical relevance of novel imaging technologies for sentinel lymph node identification and staging. *Biotechnol. Adv.* **2014**, *32* (2), 269−79.

(14) Tummers, Q. R.; Hoogstins, C. E.; Peters, A. A.; de Kroon, C. D.; Trimbos, J. B.; van de Velde, C. J.; Frangioni, J. V.; Vahrmeijer, A. L.; Gaarenstroom, K. N. The Value of Intraoperative Near-Infrared Fluorescence Imaging Based on Enhanced Permeability and Retention of Indocyanine Green: Feasibility and False-Positives in Ovarian Cancer. *PLoS One* **2015**, *10* (6), No. e0129766.

(15) Zhu, B.; Sevick-Muraca, E. M. A review of performance of near-infrared fluorescence imaging devices used in clinical studies. *Br. J. Radiol.* **2015**, *88* (1045), 20140547.

(16) Weissleder, R. A clearer vision for in vivo imaging. *Nat. Biotechnol.* **2001**, *19* (4), 316−7.

(17) Garland, M.; Yim, J. J.; Bogyo, M. A Bright Future for Precision Medicine: Advances in Fluorescent Chemical Probe Design and Their Clinical Application. *Cell Chem. Biol.* **2016**, *23* (1), 122−36.

(18) Weissleder, R.; Tung, C. H.; Mahmood, U.; Bogdanov, A., Jr In vivo imaging of tumors with protease-activated near-infrared fluorescent probes. *Nat. Biotechnol.* **1999**, *17* (4), 375−8.

(19) Whitley, M. J.; Cardona, D. M.; Lazarides, A. L.; Spasojevic, I.; Ferrer, J. M.; Cahill, J.; Lee, C. L.; Snuderl, M.; Blazer, D. G., 3rd; Hwang, E. S.; Greenup, R. A.; Mosca, P. J.; Mito, J. K.; Cuneo, K. C.; Larrier, N. A.; O'Reilly, E. K.; Riedel, R. F.; Eward, W. C.; Strasfeld, D. B.; Fukumura, D.; Jain, R. K.; Lee, W. D.; Griffith, L. G.; Bawendi, M. G.; Kirsch, D. G.; Brigman, B. E. A mouse-human phase 1 co-clinical trial of a protease-activated fluorescent probe for imaging cancer. *Sci. Transl. Med.* **2016**, *8* (320), 320ra4.

(20) Whitney, M.; Savariar, E. N.; Friedman, B.; Levin, R. A.; Crisp, J. L.; Glasgow, H. L.; Lefkowitz, R.; Adams, S. R.; Steinbach, P.; Nashi, N.; Nguyen, Q. T.; Tsien, R. Y. Ratiometric activatable cell-penetrating peptides provide rapid in vivo readout of thrombin activation. *Angew. Chem., Int. Ed.* **2013**, *52* (1), 325−30.

(21) Sakabe, M.; Asanuma, D.; Kamiya, M.; Iwatate, R. J.; Hanaoka, K.; Terai, T.; Nagano, T.; Urano, Y. Rational design of highly sensitive fluorescence probes for protease and glycosidase based on precisely controlled spirocyclization. *J. Am. Chem. Soc.* **2013**, *135* (1), 409−14.

DOI: 10.1021/acs.molpharmaceut.7b00822
Mol. Pharmaceutics XXXX, XXX, XXX−XXX

(22) Ofori, L. O.; Withana, N. P.; Prestwood, T. R.; Verdoes, M.; Brady, J. J.; Winslow, M. M.; Sorger, J.; Bogyo, M. Design of Protease Activated Optical Contrast Agents That Exploit a Latent Lysosomotropic Effect for Use in Fluorescence-Guided Surgery. *ACS Chem. Biol.* **2015**, *10* (9), 1977−88.
(23) Egeblad, M.; Werb, Z. New functions for the matrix metalloproteinases in cancer progression. *Nat. Rev. Cancer* **2002**, *2* (3), 161−74.
(24) Parks, W. C.; Wilson, C. L.; Lopez-Boado, Y. S. Matrix metalloproteinases as modulators of inflammation and innate immunity. *Nat. Rev. Immunol.* **2004**, *4* (8), 617−29.
(25) Mohamed, M. M.; Sloane, B. F. Cysteine cathepsins: multifunctional enzymes in cancer. *Nat. Rev. Cancer* **2006**, *6* (10), 764−75.
(26) Aggarwal, N.; Sloane, B. F. Cathepsin B: multiple roles in cancer. *Proteomics: Clin. Appl.* **2014**, *8* (5−6), 427−37.
(27) Oresic Bender, K.; Ofori, L.; van der Linden, W. A.; Mock, E. D.; Datta, G. K.; Chowdhury, S.; Li, H.; Segal, E.; Sanchez Lopez, M.; Ellman, J. A.; Figdor, C. G.; Bogyo, M.; Verdoes, M. Design of a highly selective quenched activity-based probe and its application in dual color imaging studies of cathepsin S activity localization. *J. Am. Chem. Soc.* **2015**, *137* (14), 4771−7.
(28) Verdoes, M.; Oresic Bender, K.; Segal, E.; van der Linden, W. A.; Syed, S.; Withana, N. P.; Sanman, L. E.; Bogyo, M. Improved quenched fluorescent probe for imaging of cysteine cathepsin activity. *J. Am. Chem. Soc.* **2013**, *135* (39), 14726−30.
(29) Olson, O. C.; Joyce, J. A. Cysteine cathepsin proteases: regulators of cancer progression and therapeutic response. *Nat. Rev. Cancer* **2015**, *15* (12), 712−29.
(30) Gocheva, V.; Wang, H. W.; Gadea, B. B.; Shree, T.; Hunter, K. E.; Garfall, A. L.; Berman, T.; Joyce, J. A. IL-4 induces cathepsin protease activity in tumor-associated macrophages to promote cancer growth and invasion. *Genes Dev.* **2010**, *24* (3), 241−55.
(31) Mordon, S.; Desmettre, T.; Devoisselle, J. M.; Soulie, S. Fluorescence measurement of 805 nm laser-induced release of 5,6-CF from DSPC liposomes for real-time monitoring of temperature: an in vivo study in rat liver using indocyanine green potentiation. *Lasers Surg. Med.* **1996**, *18* (3), 265−70.
(32) Chauhan, S. S.; Goldstein, L. J.; Gottesman, M. M. Expression of cathepsin L in human tumors. *Cancer Res.* **1991**, *51* (5), 1478−81.
(33) Jiang, J. X.; Keating, J. J.; Jesus, E. M.; Judy, R. P.; Madajewski, B.; Venegas, O.; Okusanya, O. T.; Singhal, S. Optimization of the enhanced permeability and retention effect for near-infrared imaging of solid tumors with indocyanine green. *Am. J. Nucl. Med. Mol. Imaging* **2015**, *5* (4), 390−400.
(34) Akorn Description of Clinical ICG Usage. http://akorn.com/documents/catalog/sell_sheets/17478-701-02.pdf.
(35) Intrace Description of ICG-NHS ester. http://www.intrace-medical.com/probe-boutique/icg_nhs_ester_probe_description/.
(36) Thermo Fisher Description of Dylight 780-B1 NHS Ester. https://www.thermofisher.com/order/catalog/product/53064.
(37) Philip, R.; Penzkofer, A.; Baumler, W.; Szeimies, R. M.; Abels, C. Absorption and fluorescence spectroscopic investigation of indocyanine green. *J. Photochem. Photobiol., A* **1996**, *96* (1−3), 137−148.

DOI: 10.1021/acs.molpharmaceut.7b00822
Mol. Pharmaceutics XXXX, XXX, XXX−XXX